Invention Journal of Research Technology in Engineering & Management (IJRTEM)
ISSN: 2455-3689
www.ijrtem.com Volume 2 Issue 11 ǁ November 2018 ǁ PP 57-66

Equilibrium Studies on a Chi Phase-Strengthened Ferritic Alloy

[1]ifeoma Agatha Ijomah, [2]victor Ugochukwu Nwoke and [3]franklin Amechi Anene, [4] Patrick Sunday Aguh [5]cynthia Chikodi Daniel – Mkpume

[1,] Department of Metallurgical and Materials Engineering,
[3,] Nnamdi Azikiwe University, P.M.B. 5025, Awka, Anambra State, Nigeria.
[4,] Department of Industrial Production Engineering Nnamdi Azikiwe University, P.M.B. 5025, Awka, Anambra State, Nigeria.
[5,] Department of Metallurgical and Materials Engineering University of Nigeria, Nuskka.

I. INTRODUCTION

The phase relationships for a quaternary ferritic alloy with promising high temperature properties were investigated. The alloy of interest has the composition Fe-13 pct Cr-1.5 pct Mo-3.5 pct Ti and owes its high temperature strength to the presence of a Chi phase precipitate, A "quasi binary" section representing the phase equilibria up to 1250^{o}C is proposed on the basis of evidence from microprobe, thermal analysis, metallographic and X-Ray examinations. There is a marked temperature dependence in the solid solubility of the Chi phase in the ferrite matrix which becomes particularly pronounced above 1000^{o}C. An eutectic horizontal has been identified at 1325^{o}C.

The Chi phase exhibits a wide range of stoichiometry, extending from the ternary Chi phase. $Fe_{36}Cr_{12}Mo_{10}$ to $Fe_{36}Cr_{12}Mo_3Ti_7$ accompanied by a regular increase in lattice parameter and a decrease in the solidus temperature from 1455 to 1350^{o}C. FERRITIC alloys with improved high temperature properties are of interest for use in a number of applications such as cladding and duct materials and steam generator components for liquid metal-cooled fast reactors, pressure vessels for coal gasification, heat exchangers and tubing for high temperature gas-cooled reactors, and reactor tubes for petrochemical refining.

A number of ferritic alloys based on the addition of chromium and molybdenum have been, reported[1] to have improved strengths at elevated temperatures, and better corrosion resistance and resistance to stress corrosion cracking and temper embrittlement than carbon steels[1]. Major emphasis has been on the 2 1/4 Cr-l-Mo and 9 Cr-I Mo alloys. The main impetus behind the development of high strength ferritic alloys is their appreciably lower materials cost than that of the austenitic steels or nickel-base alloys now in use in most high temperature applications.

Efforts to improve the properties of ferretic steels involve modifications in the chromium and/or molybdenum compositions and the addition of other components. Huet and coworkers[4] have developed a Chi phase-strengthened ferritic alloy with a rupture strength comparable to that of type 316 austenitic stainless steel at 700^{o}C. This ferritic alloy has the composition Fe-13 pct Cr-1.5 pct Mo-3.5 pct Ti stabilized by the addition of 2 pct TiO_2 or 1 pct Y_2O_3. At 500^{o}C and above the elongation of neutron-irradiated 316 SS decreases to 2.5 pct[5] whereas the "Huet" alloy exhibits an elongation of 5 pct at the same temperature after irradiation. Simulation tests indicate that the alloy is considerably more resistant to irradiation swelling than 316 SS and exhibits excellent resistance to corrosion by liquid sodium.

The excellent high temperature stress-rupture properties of the quaternary alloy is attributed to the formation of a Chi (or *x*) phase precipitate the high temperature microstructure of which is stabilized by the oxide dispersoid. Inasmuch as the precipitation of the *x* phase subsequent to solution treatment and hot working at 1000°C is the principal strengthening feature of the "Huet" alloy, this investigation was undertaken to determine the equilibrium compositions of the Chi and ferrite phases as a function of temperature and also to study the effect of varying the Ti :Mo ratio of the *x* phase on some of its properties. Assuming that the oxide dispersion is chemically inert phase in this alloy, it was omitted from the equilibrium studies thus simplifying the preparation of the specimens and the interpretation of their structures.

II. EXPERIMENTAL PROCEDURES

Alloy Preparation and Analysis: The iron used in this study was obtained from science equipment shop at Presidental Road Enugu in the form of electrolytic platelets with a reported purity of 99.94 pct. The chromium was iodide-refined metal of 99.99 pct, molybdenum of 99.98 pct purity and the titanium was iodide-refined material having an analyzed purity of approximately 99.95 pct were all bought from Head Bridge Market at Onitsha, Anambra State. The titanium and molybdenum contents of the *x* phase were varied interdependently from the ternary *x* phase $Fe_{36}Cr_{12}Mo_{10}$ to the stoichiometry $Fe_{36}Cr_{12}Ti_{10}$ as listed in Table I (alloys 1 to 11). The effects of variations in the Mo : Ti ratio on the lattice parameter, microstructure, melting temperature and hardness of the *x* phase were determined. Two-phase alloys with total Cr + Mo + Ti contents of 19.3, 23.0 and 25.4 at pct identified as alloys 12, 13 and 14 respectively, were used to determine the *a* and *x* boundaries. The composition of alloys 13 and 14 were arrived at from the analyzed compositions of the equilibrium phases of the 900°C isotherm for the Huet alloy (alloy 12) by increasing the amount of *x* so that the alloys lie well within the *a* + *x* field. Alloy 15 containing 27.8 at. pct Cr + Mo + Ti lies very close to the analyzed composition of the *x* boundary at 700 to 1000°C where the composition is virtually temperature independent.

Table I. Compositions of Alloys used in investigation

		Nominal Composition, Wt Pct				Analyzed Composition, Wr Pct					Intended stoichiometry of
Alloy No.	Phase(s)	At pct Fe	Cr	Mo	Ti	Fe	Cr	Mo	Ti	∑Cr + Mo + Ti	*x* phase
I	*X*	55.9	17.4	26.7	-	56.4	17.4	26.2	0		$Fe_{36}Cr_{12}Mo_{10}$
2	*X*	56.7	17.6	24.4	13.4						$Fe_{36}Cr_{12}Mo_9\ Ti_1$
3	*X*	57.5	17.8	21.9	2.8						$Fe_{36}Cr_{12}Mo_8\ Ti_2$
4	*X*	583	18.0	19.5	4.2						$Fe_{36}Cr_{12}Mo_7\ Ti_3$
5	*X*	59.2	18.3	169	5.6						$Fe_{36}Cr_{12}Mo_6\ Ti_4$
6	*X*	60.0	18.6	14.3	7.1						$Fe_{36}Cr_{12}Mo_5\ Ti_5$
7	*X*	60.8	18.9	11.6	8.7	60.8	19.4	11.7	8.1		$Fe_{36}Cr_{12}Mo_4\ Ti_6$
8	*X*	61.7	19.2	8.8	10.3					37.9	$Fe_{36}Cr_{12}Mo_3\ Ti_7$
9	*X*	62.6	19.4	6.0	12.0						$Fe_{36}Cr_{12}Mo_2\ Ti_8$
10	*X*	63.6	19.7	3.1	13.6						$Fe_{36}Cr_{12}Mo_1\ Ti_9$
11	*X*	64.6	20.0	-	15.4						
I2(Huet)	a + *X*	82.0	13.0	1.5	3.5	82.1	13.0	16	3.3	19.3	
13	a-t- *X*	78.0	13.6	1.8	6.6					23.0	
14	a + *X*	75.8	13.9	2.2	S.I					25.4	
15	~ *X*	73.4	14.4	2.8	9.4					27.8	$Fe_{42}Cr_9Mo_1\ Ti_6$

All of the alloys listed in Table I were arc melted into 35g buttons under an inert gas atmosphere. Care had to be exercised during melting to prevent loss of metal by volatilization or splattering and to eliminate cracking of the brittle x phase due to thermal shock upon rapid cooling. Three alloys designated as 1, 7 and 12 in Table 1 were submitted for chemical analysis. Comparison of the nominal and analyzed compositions in the same table indicate that the actual compositions were well within the expected ranges for all components. On the basis of these results nominal compositions have been used for the remainder of the specimens in this study.

III. SOLIDUS DETERMINATION

The solidus temperatures were determined by observing with an optical pyrometer the onset of melting in a small "black-body" hole drilled into the specimens. Alloy 12 was heated by passage of a current through the bar and the solidus was taken as the temperature at which liquid first appeared in the hole. Because of the difficulty of fabricating bars from those alloys containing significant amounts of the brittle Chi phase, small pieces of each of the other alloys were heated in a tantalum tube furnace until melting was observed by a sudden change in emissivity of the sight hole. Differential thermal analyses using a Pt-Pt/13 pct Rh thermocouple were used to determine the solidus temperatures of the "Huet" alloy and of $Fe_{36}Cr_{12}Mo_{10}$ (alloy 1). A point on the solvus of alloy 12 was also detected by DTA.

Heat Treatment and Metallography : All specimens were homogenized in a tantalum resistance furnace at 1100°C for 24h under a pressure of 10^{-6} Torr. Samples of alloy 12 were then equilibrated under the following conditions: 700°C for 250 h, 750°C for 200 *h*, 800°C for 150 h, 900°C for 120 h, 950°C for 96 h and 1000 and 1050°C for 24 h. Alloy 13 was similarly equilibrated at 800, 900 and 1000°C and alloys 13, 14 and 15 were held at 1150 and 1250°C for 24 to 96 h. The high temperature anneals at 1100°C and above were carried out in an argon atmosphere to avoid vaporization losses of chromium and. titanium. Following each of the above heat treatments the specimens were quenched in oil.

All of the alloys were electropolished in a methanol-6 pct perchloric acid solution at -70°C at a current density of 0.2 amp/cm^2 followed by an electroetch in a 10 pct oxalic acid solution. Photomicrographs of the quenched samples taken at a magnification of 250 times were used in the quantitative metallography studies.

Microprobe Analysis: Specimens of the *a + x* phase alloys that had been quenched from the different temperatures were analysed by the electron microprobe to determine the compositions of the phases present. These results together with the quantitative metallography measurements are the primary basis for the proposed "quasi-binary" section.

X-Ray Diffraction: X-Ray powder patterns of the *x* phase alloys were taken with a Debye-Scherrer powder camera, using vanadium-filtered chromium K_a radiation. The two-phase alloys (alloys 12 to 15) were studied by a diffractometer method using iron K_a radiation. Lattice parameters were obtained by the use of the Nelson-Riley function with a computer program written by Vogel and Kerapter[7].

IV. PRESENTATION AND INTERPRETATION OF RESULTS

The "Quasi-Binary'' Section: A proposed "quasi-binary" section for the quaternary system is shown in Fig. 1. This is based on the results of microprobe analyses, quantitative metallography, lattice parameter measurements, differential thermal analyses and solidus determinations of alloy 12 through 15. Because of the difficulty of describing a four-component system by a two-dimensional diagram, the sum of the alloying components at. pct Cr + Mo + Ti is plotted as a function of temperature.

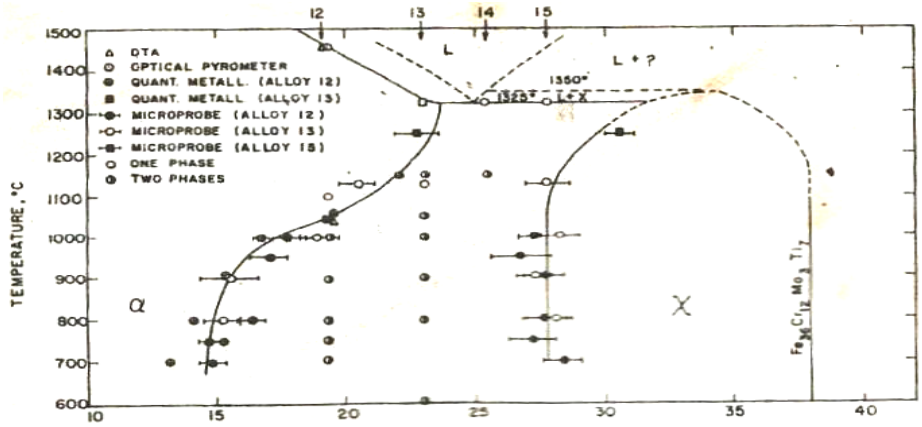

Fig. l-Proposed "quasi-binary" section of the Fe =- Cr – Mo - Ti quaternary system.

Attempts to represent this as a Fe-*x* quasi-binary section were unsuccessful however, since the x phase does not appear to be congruently soluble in *a.* However, if one plots *the* sum of the alloying components, the relative amounts of the two phases exhibit binary behavior, even though the compositions of the individual components do not vary with temperature in a true quasi-binary manner.

Microprobe Analyses: Data obtained from the microprobe analyses for alloys 12 and 13 (Table II) indicate that the iron-rich, *x*-phase boundary remains essentially constant with temperature between 700 and 1000°C, but appears to deviate rather significantly at higher temperatures. This is also evident from Fig. 1 at least within the error limits of the analyses. The error bars on the figure correspond to the sum of the errors in the analyses for the individual components and is generally on the order of ±0.5 at, pct. The data indicate a strong temperature dependence for the α solvus with a large inflection above 1000°C. The decrease in solubility that occurs between 1050 and 800°C is primarily responsible for the unusual . strengthening- that can be attained in the "Huet" alloy.

It should be noted that the points on the *a* and x phase boundaries for the synthesized alloy 13 agree with those obtained for alloy 12 at 800, 900 and l000°C. This supports the assumption that they both lie in the same binary section and hence that the higher temperature data from alloys 13 and 14 gave a valid extrapolation of the solid solubility boundaries above l000°C.

Lattice Parameter Measurements: The room temperature lattice parameters of the two-phase alloys quenched from different temperatures are shown in Fig. 2. As the quenching temperature is increased from 700 to 1250°C the lattice parameter of the *α* matrix increases from 2.873 to 2.91Å. The parameter of the *x* phase remains constant at 8.864Å between 700 and 1050°C (identical for alloys 12, 13 and 15) but increases at the higher temperatures. This is indicative of a deviation from the temperature independence of the *x* phase boundary above 1050° C in agreement with the microprobe results and metallographic evidence. The microprobe analyses place the composition of the saturated *x* phase at 1050°C and below as $Fe_{42}Cr_9Mo_1Ti_6$. This is in disagreement with the results of Huet and Leroy[4] who reported a stoichiometry of $Fe_{36}Cr_{12}Mo_3Ti_7$ for this phase. The lattice parameter of an alloy of the latter stoichiometry was determined in the present investigation to be 8.946 ± 0.004Å, much higher than the value of 8.864 obtained for the saturated *x* phase. Since the iron content of $Fe_{42}Cr_9Mo_1Ti_6$ is considerably higher and the chromium, molybdenum and titanium contents lower than for $Fe_{36}Cr_{12}Mo_3Ti_7$, the discrepancy in the lattice parameters can readily be explained on the basis of differences in atomic size. As the smaller iron atoms (atomic radius - 1.241Å) substitute for the larger chromium (1.249Å), molybdenum (1.363Å) or titanium (1.432Å) atoms in the *x*-phase lattice the dimensions of the unit cell should decrease.

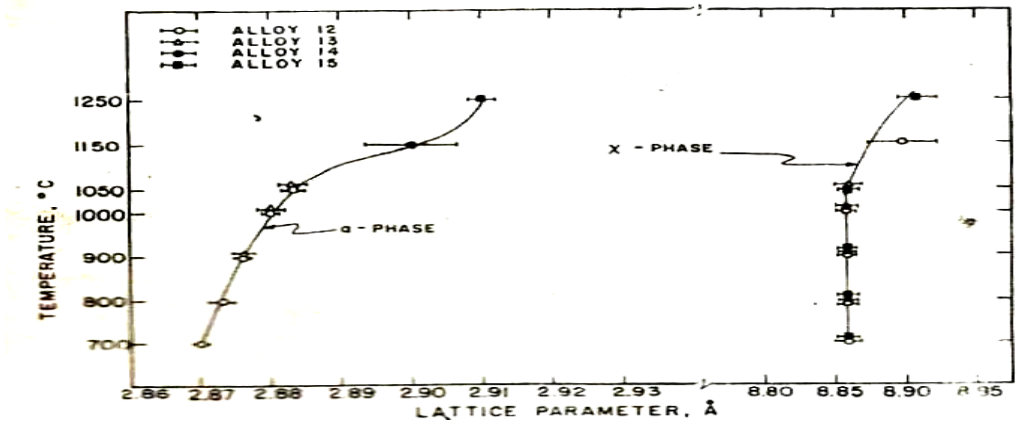

Fig. 2—Variation of room temperature lattice parameters of *α* and *x* phases with quench temperature.

Table II. Microprobe Analysis Results of *x and a Phases*

Alloy	Temperature, °C	Heat Treatment, h	*x* Phase, At. Pct*				a Matrix, At. Pct			
			Cr	Mo	Ti	Σ	Cr	Mo	Ti	S
12	700	250	15.0	1.5	11.9	28.4	13.6	0.2	1.0	14.8
12	750	200	14.7	1.4	11.1	27.2	13.2	0.2	1.2	14.6
12	800	150	15.9	2.0	10.1	28.0	14,1	0,5	1.7	16.3
13	800	150	15.7	1.4	10.6	27.7	13,0	0.2	2.0	15.2
12	900	120	15.2	1.5	11,0	27.7	13.6	03	1.8	15.7
13	900	120	15.8	1.2	10.4	27.4	13.1	03	2.1	15.5
12	950	96	14.4	1.3	11.0	26.7	14. 1	05	2.4	17.0
12	1000	24	15.4	1.7	10.1	27.2	14.5	0.7	2.4	17.6
13	1000	24	15.5	1.8	10.8	28.1	15.4	0.7	2.7	18.8
13	1130	24	14.3	1.5	11.9	27.7	14.5	0.5	5.1	20.4
15	1250	96	16.3	1.6	I2.S	30.7	17.8	1.6	3.3	22.7

* The average errors in the microprobe analyses are: Cr ± *0.2* pct, Mo ± 0.1 pct, Ti ± 0.2 pct in *x* phase and Ti ± 0.03 pct in a phase.

Metallographic Examination: The amount of precipitate in the quenched samples of alloys 12 through 15 was estimated by the grid method of fractional estimation, as is seen from Table III. Points on the α-phase boundary were determined from these results by application of the lever rule. This treatment assumed that the location of the *x* boundary was that obtained from the microprobe analyses and that it was temperature invariant over most of the temperature range. As is seen from the plotted points on Fig. 1 there is fairly good agreement between the quantitative metallography and microprobe results for the α-solvus. Micro structures of alloy 12 as quenched from 1050 and 700°C are shown in Fig. 3. A comparison of these reveals a change from one phase at 1050° C to a microstructure containing significant amounts of *x* precipitate at 700°C. A similar sequence for alloy 13 shows a marked decrease in the amount of *x* as the quench temperature is increased from just below the inflection in the solvus at 1000°C to above it at 1130°C (Fig. 4).

The recession in the x phase boundary above 1100°C is indicated by the microprobe and lattice parameter results and supported by microstructural evidence which shows a definite increase in the amount of *a* present in the 27.8 at. pct alloy (15) between 1000°C at which temperature it is nearly one phase and 1250°C where it contains about 25 pct α (Fig. 5).

Solidus and Solvus Boundaries: Solidus data obtained by the optical pyrometer and differential thermal analyses methods are shown in Table IV. An eutectic horizontal at 1325°C, and a peritectic lying just above it at 1350°C are proposed on the basis of thermal analyses and microstructural evidence. The coincidence of the melting points of alloys 13, 14 and 15 as seen from Fig 1 suggests the presence of an eutectic horizontal at about 1325°C. This is supported by the microstructures of the rapidly-cooled liquid phase in alloy 14 (Fig. 6) formed during the melting point determinations which places the eutectic close to the composition of that alloy. A greatly magnified view of the eutectic is seen from the SEM micrograph shown in Fig. 7.

Table III. Quantitative Metallography Data

Alloy	Heat Treatment Temperature, °C	Time, h	Pet of *x* Phase in Alloy
12	700	250	42
12	750	200	33
12	800	150	38
12	900	120	32
12	950	96	28
12	1000	24	25
12	1030	77	10
13	1000	77	57
13	1050	90	40
13	1130	24	32
13	1250	24	29
14	1150	88	59
15	1000	77	98
15	1250	96	76

Table IV: Solvus and Solidus Determination

Alloy	Phase boundary	Method of Determination	Temperature, °C
12	Solidus	Optical Pyrometer	1450
12	Solidus	DTA	1445
12	Solvus	DTA	1050
13	Solidus	Optical Pyrometer	1325
14	Solidus	Optical Pyrometer	1325
15	Solidus	Optical Pyrometer	1325

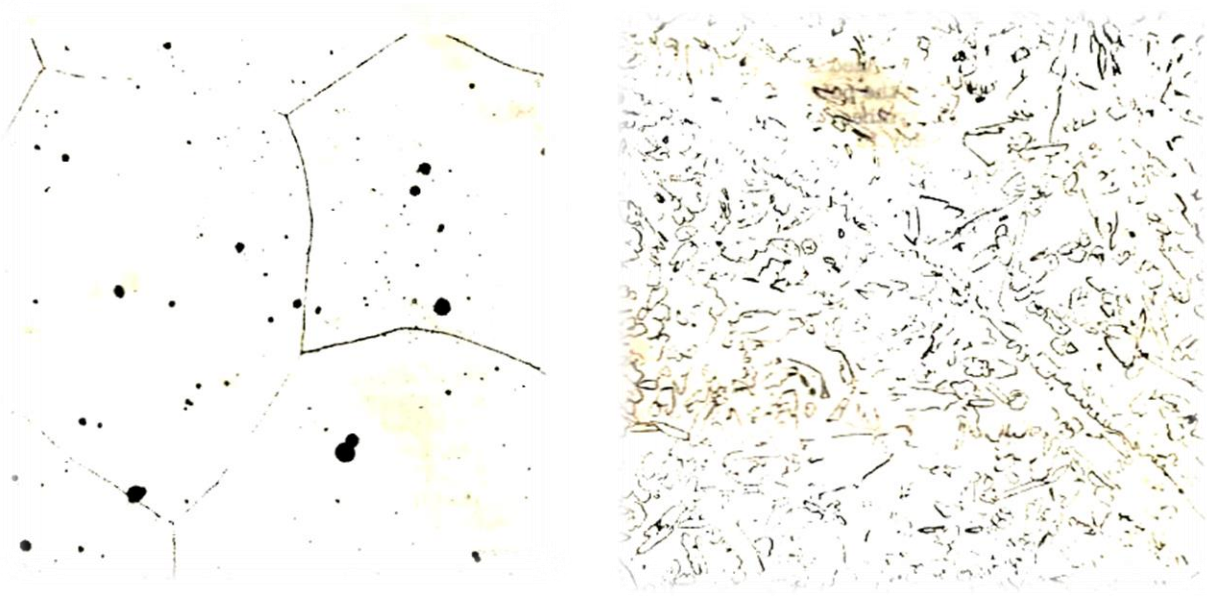

(a) (b)

Fig. 3—Huet alloy (alloy 12) quenched from above and below the α solvus temperature. Electrolytic etch. Magnification 275 times, *(a)* Quenched from 1050°C showing single phase *a* structure, (b) Quenched from 700°C showing x phase precipitate in α matrix.

Evidence for the occurrence of a peritectic horizontal at approximately 1350°C is somewhat less conclusive. It rests primarily on the microstructures of alloys 14 and 15 both of which show three-phase microstructures upon melting. . This is illustrated by Fig. 6 in which a peritectic rim appears to surround the primary crystals.

The solidus temperature was determined for alloy 12 by the optical pyrometer and DTA methods. There is good agreement between the two methods which gave values of 1450 and 1445°C respectively. A thermal arrest at 1050°C corresponding to a point of the inflection region of the α solvus was detected by the DTA method. This is in agreement with the micro-structural evidence which places the boundary between 1050 and 1000°C (Fig. 1) at this composition.

in α p
ct X i

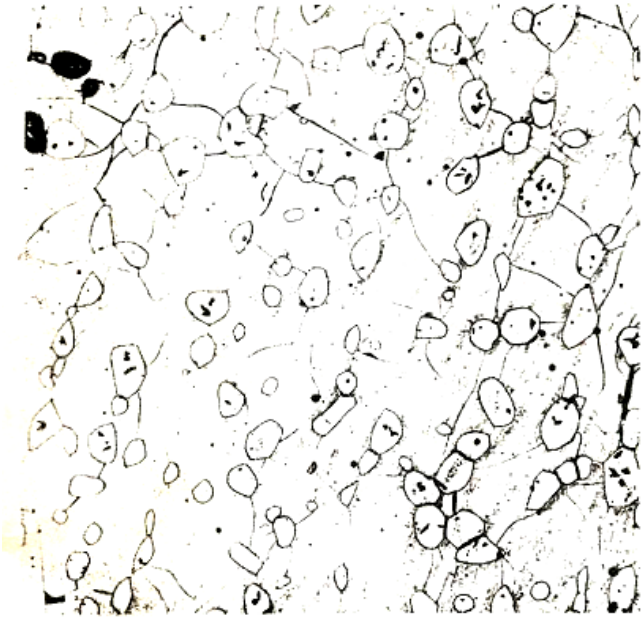

Fig. 5 - Alloy 15 quenched from 1250°C showing α in *x* matrix indicative of a receding *x* phase boundary at higher temperatures. Electrolytic etch. Magnification 275 times.

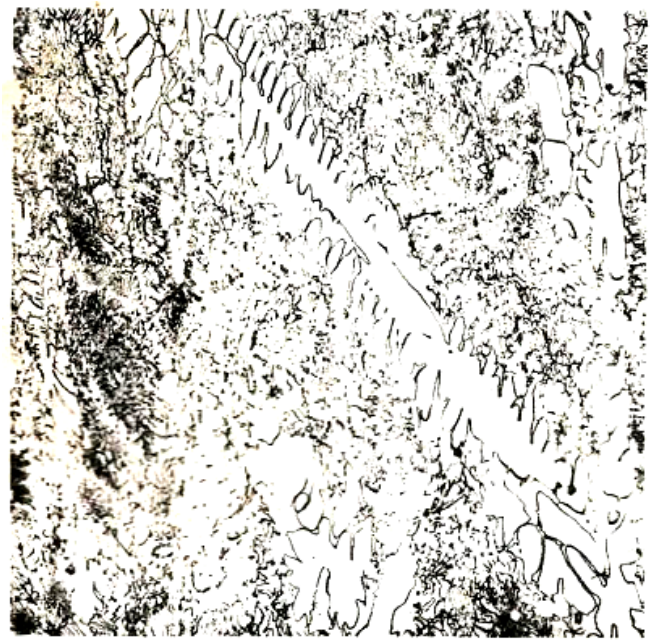

Fig. 6 - Alloy 14 rapidly cooled from its melting point. Shows peritectic rim of *x* surrounding unidentified primary phase plus eutectic mixture. Electrolytic etch. Magnification 275 times.

The $Fe_{36}Cr_{12}Mo_xTi_{10-x}$ System *(*x = 0. . . 10)

Huet *et al*[4] report that a *x* phase of the approximate stoichiometry, $Fe_{36}Cr_{12}Mo_3Ti_7$ was the precipitate in the Fe-13 Cr-1.5 Mo-3.5 Ti quaternary ferritic alloy and that this was primarily responsible for the superior strength of the alloy at elevated temperatures. This appears to be a modification of the well-known ternary Chi phase, $Fe_{36}Cr_{12}Mo_{10}$ (Refs. 9, 11) by substitution of titanium for molybdenum in the lattice. The purpose of this portion of the work was to determine the extent to which titanium can replace molybdenum in the *x* phase structure by investigating the $Fe_{36}Cr_{12}Mo_{10-x}Tix$ (x = 0, 1, 2 … 10) section.

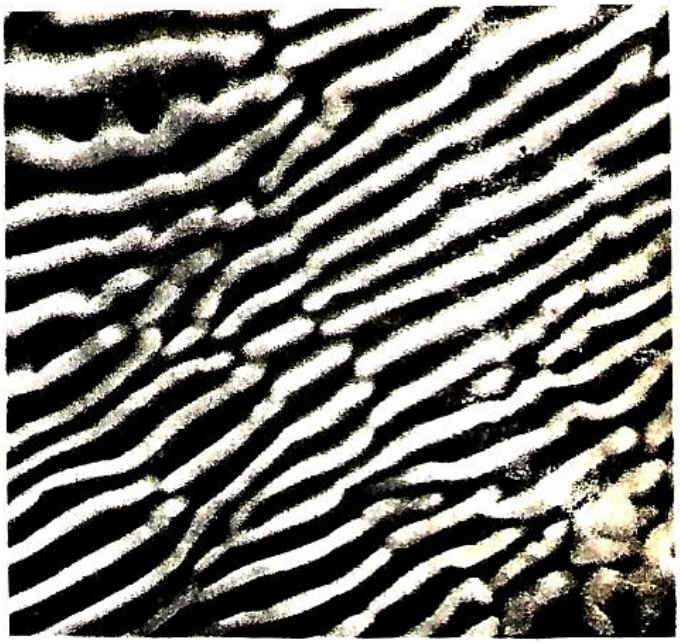

Fig. 7—SEM picture of eutectic region. Magnification 5830 times.

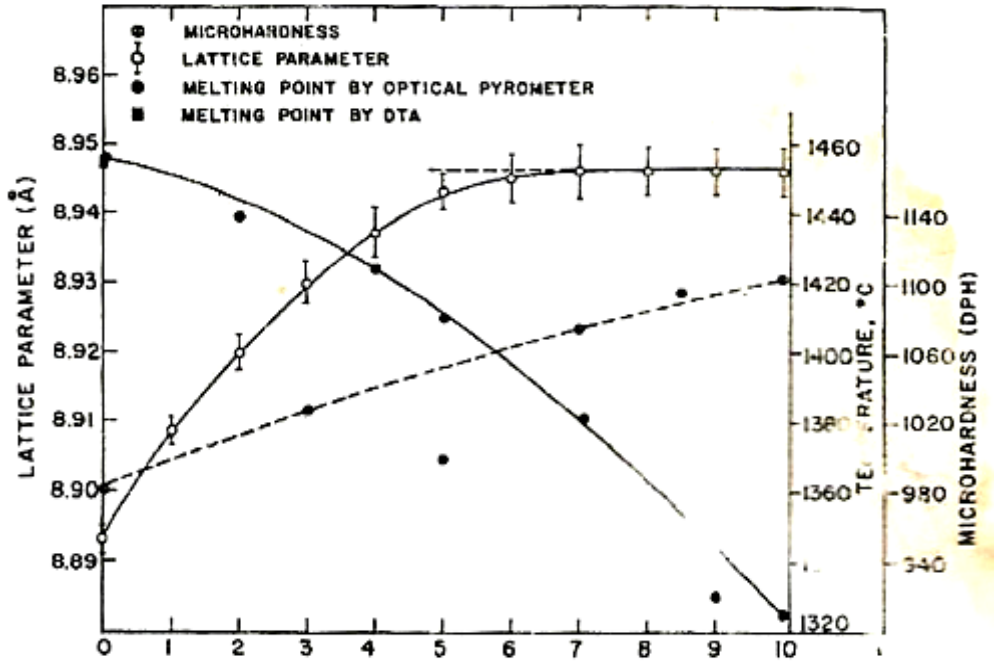

Fig. 8 - Variation of lattice parameter, melting point and microhardness with moles of Ti in the $Fe_{36}Cr_{12}Mo_{10}Ti_x$ system.

The melting points, lattice parameters, micro-structures and microhardnesses were determined as a function of the Mo: Ti ratio.

Solid Solubility Limit: A plot of lattice parameter *vs* the number of atoms of titanium per unit cell is shown in Fig. 8. The plot indicates that the lattice parameter of the *x* phase increases monotonically as molybdenum is replaced by titanium up to = 7. This places the solubility limit very close to the Ti:Mo ratio of 7:3. This is supported by the microstructures of the nearly single-phase alloy, $Fe_{36}Cr_{12}Mo_{10}Ti_7$ shown in Fig. 9.

A lattice parameter of 8.893Å was obtained for the ternary Chi phase, $Fe_{36}Cr_{12}Mo_{10}$. This is in agreement with the work of Koh[8] who reported 8.89Å and with the later work of Takeda and Yukawa[9] who obtained a value of 8.90A, but differs somewhat from the value of 8.92A by McMullin *et al*[10].

Pearson[11] reports the existence of a ternary Chi phase having a stoichiometry of approximately $Fe_{34}Cr_{15}Ti_9$ with a lattice parameter of 8.922Å. This is in contrast to the two-phase ternary alloy, $Fe_{36}Cr_{12}Ti_{10}$, of the present investigation in which the *x* phase has a lattice parameter of 8.946Å, It will be noted, of course, that Pearson's phase has a higher chromium and lower iron and titanium content than that attempted here which probably accounts for the difference in the cell dimension and microstructures of the two stoichiometries.

Solidus : The results of the solidus determinations for the series of *x* phase alloys are plotted in Fig. 8. The data show a regular lowering of the melting point of the *x* phase as the higher melting molybdenum (T_m = 2620ºC) is replaced by titanium (T_m = 1660°C).

Microhardness: The hardness of the *x* phase alloys increases from 980 DPH at $x = 0$ to 1100 at $x = 10$ as is seen from Fig. 8. The anomalously low value at 5 atoms of titanium appears to be real since it was reproduced on duplicate alloys.

V. DISCUSSION

The discrepancy between the composition of the saturated *x* phase reported by Huet and coworkers as $Fe_{36}Cr_{12}Mo_3Ti_7$ and that obtained from this investigation, $Fe_{42}Cr_9Mo_1Ti_6$ is worthy of further consideration. The principal difference between the two studies was the method of alloy preparation. Huet's study involved the use of powder metallurgy techniques and the addition of an oxide dispersion whereas our study was done on arc-melted alloys with no oxide addition. Although TiO_2 is thermodymmically more stable than the oxides of the other metallic elements in the alloy it is possible that under certain conditions TiO_2 could react with one of the components of the alloy thus altering the compositions of the phases and the position of the boundaries. One of the problems encountered in the long time equilibration treatments at the higher temperatures was the loss of titanium. After 72 h at 1250°C measureable weight losses and the appearance of a depleted diffusion zone near the surface were observed. Microprobe analyses indicated that this was due primarily to the loss of titanium from this region. Thus, the time at temperature above 1100°C was determined by the minimum time required to attain equilibrium.

It would have been more elegant if the proposed diagram could have been represented as a true quasi-binary section of the Fe-*x* system. Although the system exhibits many of the features of a binary system there is no single stoichiometry of x which when added to iron describes the quaternary composition of the *a* solvus at all temperatures. The use of the total solute concentration *vs* temperature relationship gives a "quasi-binary" type of behavior as is seen from the rather good agreement between the quantitative metallography and micro-probe analysis results.

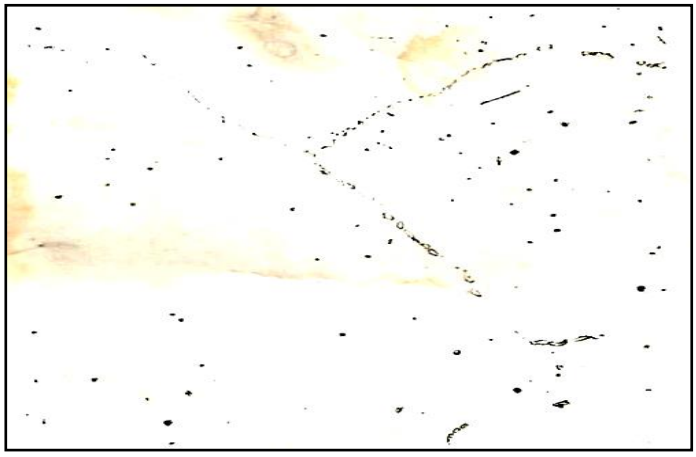

Fig. 9 – Microstructure of $Fe_{36}Cr_{12}Mo_3Ti_7$ showing the presence of small amounts of second phase in *x* phase grain boundaries. Electrolytic etch. Magnification 275 times.

SUMMARY

1) A "quasi-binary" phase diagram with the follow ing features has been proposed:
   a) An eutectic at 1325ºC and about 22 at. pct Cr + Mo + Ti.
b) An inflection in the α solvus between 1000 and 1100°C.
c) The terminal boundary of the quaternary *x* phase having the stoichiometry of $Fe_{42}Cr_9Mo_1Ti_6$ up to 1050° C.
2) A solubility limit for the quaternary *x* phase region, $Fe_{36}Cr_{12}Mo_{10-x}Ti_x$ at the Ti : Mo ratio of approximately 7:3.

REFERENCE

1. Cannon, N.S.; Hu, WL; Gelles, D.S.
2. Charpy impact test results for low-activation ferritic alloy Sci Tech connect 1987-05-07
3. A.J. McNab; Chem.Eng.Prog., 1989, Vol. 71, No 11, P 51
4. J.J Huet and V. Leroy: Nucl. Technol. 1984, Vol. 40, P. 216
5. P.Van Asbroeck, M. Snykers and W.Vandermealen: Effect of Radiation on substructure and Mechanical property of metals and alloys Vol. 582, P. 255 ASTM, STP 1989.
6. Hagel, William C.; Smidt, Fredrick A.; Korenko, Michael K.; High strength ferritic alloy DOE patents 1977-01-01.
7. F.A. Schmidt, R.M Bergmen, H.A. Wilhelm: J. Metals 1977, Vol. 23, No 8, P. 38.
8. R.E. Vogelan C.P Kempter: Acta Cystallogr.1986, Vol. 24, P. 1130.
9. P.K Koh: Trans AIME, 1983, Vol. 297, P. 339.
10. Shuzo Takeda and Natsue Yukawa: Jap J. Metals, 1977 Vol 51, Page 275.
11. J.G. McMullin, S.F. Reiter, and D.G Ebeling: Trans ASM, 1974, Vol. 66, P. 779.
12. W.B Pearson: Handbook of lattice spacings and structures of metals and alloys, Vol. 8, Pergaman press, New York, 1987.